Protein kinase C mediates up-regulation of tetrodotoxin-resistant, persistent Na^+ current in rat and mouse sensory neurones

Mark D. Baker

Molecular Nociception Group, Department of Biology, Medawar Building, University College London, Gower Street, London WC1E 6BT, UK

The tetrodotoxin-resistant (TTX-r) persistent Na^+ current, attributed to $Na_V1.9$, was recorded in small ($< 25\ \mu$m apparent diameter) dorsal root ganglion (DRG) neurones cultured from P21 rats and from adult wild-type and $Na_V1.8$ null mice. In conventional whole-cell recordings intracellular GTP-γ-S caused current up-regulation, an effect inhibited by the PKC pseudosubstrate inhibitor, PKC19–36. The current amplitude was also up-regulated by 25 μM intracellular 1-oleoyl-2-acetyl-sn-glycerol (OAG) consistent with PKC involvement. In perforated-patch recordings, phorbol 12-myristate 13-acetate (PMA) up-regulated the current, whereas membrane-permeant activators of protein kinase A (PKA) were without effect. PGE_2 did not acutely up-regulate the current. Conversely, both PGE_2 and PKA activation up-regulated the major TTX-r Na^+ current, $Na_V1.8$. Extracellular ATP up-regulated the persistent current with an average apparent K_d near 13 μM, possibly consistent with P2Y receptor activation. Numerical simulation of the up-regulation qualitatively reproduced changes in sensory neurone firing properties. The activation of PKC appears to be a necessary step in the GTP-dependent up-regulation of persistent Na^+ current.

(Resubmitted 4 May 2005; accepted after revision 6 July 2005; first published online 7 July 2005)
Corresponding author M. D. Baker: Molecular Nociception Group, Department of Biology, Medawar Building, University College London, Gower Street, London WC1E 6BT, UK. Email: mark.baker@ucl.ac.uk

Many small diameter dorsal root ganglion neurones (DRG) generate a tetrodotoxin-resistant (TTX-r) Na^+ current with very slow kinetics operating over a membrane potential range some 20 mV or more negative than the transient Na^+ currents generated in the same cell (Cummins *et al.* 1999; Baker & Wood, 2001; Dib-Hajj *et al.* 2002). It is usually referred to as the persistent current and was first recorded by Cummins *et al.* (1999) in $Na_V1.8$ null neurones, where the major portion of the TTX-r Na^+ current is missing. The current is attributed to the $Na_V1.9$ (NaN) gene known to be expressed in peripheral nociceptive neurones (e.g. Cummins *et al.* 1999; Fjell *et al.* 2000; Fang *et al.* 2002), and in myenteric neurones (Rugiero *et al.* 2002; Rugiero *et al.* 2003). Consistent with a possible role in peripheral nociception, the channel has been immunocytochemically localized to unmyelinated nerve endings in the cornea (Black & Waxman, 2002). Recently, the DRG neurones of an $Na_V1.9$ null mutant have been characterized as apparently missing the persistent TTX-r Na^+ current, and the animals show deficits in pain behaviour during the second phase of the intraplantar formalin test, suggesting that the current is necessary for prolonged activation of peripheral nociceptive endings (Priest *et al.* 2005).

Although the activation kinetics of the persistent current are too slow for it to contribute to the up-swing of an action potential, it can participate in the control of excitability because it is regenerative and operates at subthreshold membrane potentials. The current exhibits wide activation/inactivation gating overlap (e.g. Herzog *et al.* 2001), and when up-regulated can generate steady-state currents large enough to depolarize the membrane potential (Herzog *et al.* 2001; Baker *et al.* 2003). The non-hydrolysable analogue of GTP, GTP-γ-S, strongly up-regulates the current leading to spontaneous action potential generation at potentials near −60 mV (Baker *et al.* 2003). The magnitude of this up-regulation suggests that G-protein pathway modulation of the current may be functionally important. Modulation probably involves a phosphorylation step, because it is inhibited by the non-selective protein kinase inhibitor, H7 (Baker *et al.* 2003), although the kinase involved has remained uncharacterized. Substantial protein kinase A- and C-dependent modulation has been demonstrated for $Na_V1.8$, where kinase A activation causes an increase in macroscopic current amplitude and makes the voltage dependence of activation steeper, shifting the midpoint in the hyperpolarizing direction (England *et al.* 1996;

 DOI: 10.1113/jphysiol.2005.089771

Gold *et al.* 1998; Fitzgerald *et al.* 1999). Consensus site serines that have been defined in a heterologous system (Fitzgerald *et al.* 1999) are involved in these effects. Block of background kinase C activity has been found also to prevent kinase A-dependent up-regulation, whereas blockers of kinase A had no effect on the protein kinase C dependence of $Na_V1.8$ (Gold *et al.* 1998).

G-protein-coupled ATP receptors on sensory nerve may cause changes in excitability lasting longer than those attributable to the activation of P2X receptors (e.g. Molliver *et al.* 2002; Stucky *et al.* 2004). Molliver *et al.* (2002) have found that selective activation of P2Y receptors can reproduce a prolonged period of action potential firing in cultured sensory neurones observed when applying ATP, although the mechanism causing the hyperexcitability is mysterious. One possibility is that the hyeperexcitability may ensue through the up-regulation of persistent Na^+ current. The present experiments help to test this hypothesis by delineating the kinase type involved in persistent Na^+ current up-regulation and by determining whether the current can be controlled by ATP.

Methods

Tissue preparation and culturing procedures have been previously described (e.g. Baker *et al.* 2003; Baker & Bostock, 1997). The adult mice and P21 Sprague-Dawley rats used were killed in accordance with Home Office guidelines by cervical dislocation. Neurones were used within 1 or 2 days of initially plating out on poly L-lysine coated coverslips.

Solutions and electrophysiology

These experiments utilized the conventional whole-cell patch-clamp technique with membrane patch rupture and also used amphotericin-B perforated patches. The solutions for both conventional whole-cell voltage-clamp and current-clamp are detailed in Baker *et al.* (2003) with a modification in some of the present experiments, where 1-oleoyl-2-acetyl-sn-glycerol (OAG) was applied during voltage-clamp recording from wild-type (WT) neurones, EGTA was equimolarly replaced by BAPTA in the pipette solution. Normal whole-cell voltage-clamp experiments utilized the same reduced $[Na^+]$ external solution as detailed previously and also below for perforated-patch recordings. For voltage-clamp using the perforated-patch technique, the solutions used were the following (mM). External: NaCl 43.3, tetraethylammonium chloride 96.7, Hepes 10, $CaCl_2$ 2.1, $MgCl_2$ 2.12, 4-aminopyridine 0.5, CsCl 10, KCl 7.5, $CdCl_2$ 0.1, TTX 0.25×10^{-3}. Pipette: $CsMetSO_4$ 110.0 mM, CsCl 30.0 mM, $MgCl_2$ 1.0 mM, $CaCl_2$ 0.1–5.0 mM, Hepes 10 mM. Both solutions were buffered to pH 7.2–7.3 with the addition of CsOH. The pipette solution contained Ca^{2+} (0.1–5 mM) for two reasons. Firstly, the presence of Ca^{2+} seemed to improve seal formation, and secondly, the recording was lost following patch breakdown, helping to prevent recording during accidental dialysis of the cytoplasm. When almost simultaneous current-clamp and voltage-clamp recordings were made using the perforated-patch technique (see Fig. 6), $CsMetSO_4$ and CsCl were equimolarly replaced with $KMetSO_4$ and KCl, respectively, and the extracellular current-clamp solution detailed in Baker *et al.* (2003), with a normal external $[Na^+]$ was used. For perforated-patch recordings, electrode tips were filled with pipette solution without amphotericin-B, and subsequently solution containing amphotericin-B (final concentration of 200 $\mu g\,ml^{-1}$) was used to fill the electrode. In current-clamp experiments, the aim was to find whether persistent Na^+ current up-regulation could alter excitability, measured in terms of applied depolarizing current, and an estimate of voltage threshold. In order to maximize the effects of the current on excitability, the neurones were routinely held at −80 or −90 mV, so that the amount of resting inactivation of the persistent Na^+ current was low. This was achieved by applying a polarizing current, adjusted from time to time to maintain a steady membrane potential value.

Electrodes were made from thin-walled glass (Harvard Apparatus, Edenbridge, Kent, UK), and had a resistance of between 1.5 and 3 MΩ when initially filled with the pipette solution. The voltage-clamp protocols were generated using an Axopatch 2B amplifier (Axon Instruments, Union City, CA, USA) controlled by a PC running pCLAMP 9 (Axon Instruments). Series-resistance compensation was set near 70%, with a nominal feed-back lag of 12 μs for conventional whole-cell recordings and 20 μs for perforated-patch recordings. Recordings were filtered at 5 kHz (4-pole Bessel filter) and usually digitized at 10 kHz. For whole-cell recordings the holding potential was −110 mV, and incrementing clamp steps were preceded by a 20 ms duration prepulse to −130 mV (unless otherwise stated). The responses to three consecutive families of clamp steps were averaged. Leak subtraction was achieved on-line, using a *P*/*N* protocol, where five reverse polarity clamp steps were averaged to generate the leakage record. Each interstep interval was 1.5 s and the protocol repeat frequency for a 16 step protocol was 0.04 Hz. When using both the Cs^+ and K^+ perforated-patch pipette solutions, a junction-potential existed at the end of the pipette, measured as +13 mV. The junction potential was backed off at the start of recording to zero the current, but the offset disappeared on seal formation, so that subsequent holding and test potentials had to be corrected for the initial overcompensation. Following stable seal formation, the series resistance was repeatedly estimated until it fell to 10 MΩ or below (before compensation). In order to minimize problems in voltage clamp associated with the high series resistance of the perforated-patch recording,

the size of the Na^+ currents were normally reduced by using the reduced external [Na^+] solution described above. Recordings in which Na^+ current activation was not gradual with incrementing depolarization when using perforated patches, suggesting an inadequate voltage clamp, were excluded from the analysis. Conventional whole-cell recordings exhibited a substantially lower series resistance usually close to 3 MΩ before compensation.

Materials

Reagents were obtained from Sigma-Aldrich (Poole, Dorset, UK), except phorbol 12-myristate 13-acetate (PMA), which was purchased from Tocris Cookson (Bristol, UK), tetrodotoxin (TTX), purchased from Alomone Laboratories (TCS Biologicals, Botolph Claydon, Bucks, UK), and PKC 19–36, purchased from Calbiochem (Merk Biosciences Ltd, Nottingham, UK). PMA, ATP and PGE_2 solutions were applied by gravity fed local superfusion. 1-Oleoyl-2-acetyl-sn-glycerol (OAG) was incorporated into the pipette solution.

Data analysis

Peak sodium current values were converted to conductance values using the equation:

$$G = I/(V_m - E_{Na})$$

where G is the conductance, I the maximum current amplitude, V_m the membrane potential, and E_{Na} the equilibrium potential value for Na^+, given in the text. The Boltzmann equation was used to describe steady-state activation:

$$G = G_{max}/(1 + \exp(V_{½} - V_m)/a_g)$$

G_{max} is the peak conductance, $V_{½}$ is the potential at half maximal activation, and a_g is the slope factor in mV.

Where possible, data are presented as mean values ± S.E.M.

Simulations

Simulations were of a space-clamped neurone soma (run in Visual Basic on a PC, employing the Euler method with an integration time step of 1 μs), using equations and voltage-dependent kinetic parameter values modified from Herzog *et al.* (2001) and from Bostock *et al.* (1991). Three forms of Na^+ current (TTX-s, $Na_V1.8$ and persistent Na^+ current) and two types of K^+ current were included in the simulation (G_{KF}, kinetically fast K^+ channels and G_{KS}, kinetically slow K channels). The voltage-activated K^+ currents were assumed to be similar to those in myelinated axons, with shifted voltage dependence, matching the relatively depolarized voltage dependence of transient Na^+ currents in small diameter sensory neurones. In the absence of a full kinetic analysis of $Na_V1.8$, the voltage-dependent rate constants were chosen to give currents in voltage clamp exhibiting plausible kinetics and voltage dependence, and in order to generate an action potential exhibiting an inflection. The forms of the equations used to derive the rate constant values were taken from the analysis of TTX-sensitive current of Herzog *et al.* (2001). The voltage-dependent parameters provided by Herzog *et al.* (2001) for persistent Na^+ current were modified to more closely match Na^+ current recordings made using conventional whole-cell methods, without internal F^-, where the current exhibits a less negative voltage dependence than that reported by Dib-Hajj *et al.* (2002). Simulated TTX-r Na^+ currents, which provide most of the inward Na^+ current, are compared with real currents in Fig. 8. Conductance values of TTX-s Na^+ current and $Na_V1.8$ were chosen to make the fractional conductance attributable to $Na_V1.8$ substantially larger than that of TTX-s Na^+ current, appropriate for a nociceptive neurone, and analogous to nociceptive endings in the cornea and dura that retain their excitability even in the presence of micromolar concentrations of TTX (Brock *et al.* 1998; Strassman & Raymond, 1999). A minor fraction of the total TTX-s Na^+ conductance, equivalent to 2% of the transient conductance, was incorporated as a non-inactivating persistent conductance, with an activation voltage dependence 20 mV more negative than for the transient current (Kiernan *et al.* 2003; Bostock & Rothwell, 1997). The up-regulation of persistent Na^+ current was achieved simply by adding the current to a neurone first simulated without it. When the persistent conductance was set to 100 nS, it was sufficient to generate close to 4 nA peak current (i.e. in response to a voltage-clamp step to −10 mV) in simulated voltage-clamp with a one-third Na^+ gradient. This is similar to a reasonably large example of a real up-regulated current (e.g. Fig. 5*A* in Baker *et al.* 2003). Using either 15 pF or 30 pF for the neuronal capacitance did not qualitatively affect the result of incorporating a persistent Na^+ conductance. The simulation was run using room temperature parameter values.

The transmembrane ionic currents were described by the following equations:

$$\begin{aligned} I_{ion} = {} & m^3 h G_{Na}(E_m - E_{Na}) + m_p^3 G_{NaP}(E_m - E_{Na}) \\ & + m_8^3 h_8 G_{Na8}(E_m - E_{Na}) + m_9 h_9 G_{Na9}(E_m - E_{Na}) \\ & + n_F^4 G_{KF}(E_m - E_K) + n_S G_{KS}(E_m - E_K) + E_m/R_{in} \end{aligned} \quad (1)$$

$$I_{cap} = -I_{ion} \quad (2)$$

where I_{ion} is the total transmembrane ionic current and I_{cap} is the capacitative current, E_m is the membrane potential, R_{in} is the input resistance, E_{Na} and E_K are the Na^+ and K^+ equilibrium potentials, respectively.

Table 1. Values of A, B and C used to derive the values of voltage-dependent rate-constants

	A (ms^{-1})	B (mV)	C (mV)
α_m	17.235	7.58	−11.47
β_m	17.235	66.2	19.8
β_h	10.8	−11.8	−11.998
α_{mP}	17.235	27.58	−11.47
β_{mP}	17.235	86.2	19.8
α_{m8}	3.83	2.58	−11.47
β_{m8}	6.894	61.2	19.8
β_{h8}	0.61714	−21.8	−11.998
α_{m9}	1.548	−11.01	−14.871
β_{m9}	8.685	−112.4	22.9
α_{h9}	0.2574	63.264	3.7193
β_{h9}	0.53984	0.27853	−9.0933
α_h	0.23688	115	46.33
α_{h8}	0.013536	105	46.33
α_{nF}	0.00798	72.2	1.1
α_{nS}	0.00122	−10.5	23.6
β_{nF}	0.0142	55	10.5
β_{nS}	0.000739	57.1	21.8

Equation (2) holds true in a space-clamp, without longitudinal currents. m and h are the voltage-dependent activation and inactivation gating parameters for the TTX-s Na^+ current (Hodgkin & Huxley, 1952) and likewise m_8 and h_8 are the voltage-dependent activation and inactivation gating parameters for $Na_V1.8$, and m_9 and h_9 are for the persistent Na^+ current. m_P is the activation gating parameter for the persistent TTX-s Na^+ current. n_F and n_S represent the activation gating parameters for the fast and slow K^+ currents, respectively. G_{Na}, G_{NaP}, G_{Na8}, G_{Na9}, G_{KF} and G_{KS} represent the maximum conductance for transient TTX-s Na^+ current, persistent TTX-s Na^+ current, $Na_V1.8$, persistent Na^+ current, fast K^+ current and slow K^+ current, respectively.

For simulating the effects of up-regulating persistent Na^+ current on a neurone held at −90 mV in current-clamp (cf. Baker *et al.* 2003), the following fixed parameter values were used: cell capacity = 15 pF; R_{in} = 200 MΩ; E_K = −85 mV; E_{Na} = 79.6 mV; G_{Na} = 18 nS; G_{NaP} = 0.36 nS; G_{Na8} = 220 nS; G_{Na9} = 0 or 100 nS; G_{KF} = 30 nS; G_{KS} = 2 nS. In addition, a polarizing current of 454 pA was applied to maintain a holding potential of −90 mV. This was for two reasons. Firstly, this removes resting inactivation from the persistent Na^+ current, maximizing its subsequent effects on excitability, and secondly, it replicates what was done in Baker *et al.* (2003). In an attempt to simulate the generation of spontaneous activity by up-regulating persistent Na^+ current in a resting neurone (seen in current-clamped neurones at membrane potentials close to −60 mV; Baker *et al.* 2003), R_{in} was increased to 2 GΩ, giving a resting potential of −58.4 mV. The G_{Na9} conductance was increased up to 38 nS, and a hyperpolarizing 'pump-current' (indistinguishable from a small polarizing current) was simultaneously added. All other parameter values remained unchanged. The values of m, h, m_P, m_8, h_8, m_9, h_9, n_F and n_S were calculated from voltage-dependent rate constants α_x and β_x, where x indicates any single gating parameter. α_m, β_m, β_h, α_{mP}, β_{mP}, α_{m8}, β_{m8}, β_{h8}, α_{m9}, β_{m9}, α_{h9}, β_{h9} were calculated according to the formula: $A/(1 + \exp((E_m + B)/C)$. α_h and α_{h8} were given by $A\exp(-(E_m + B)/C)$. α_{nF} and α_{nS} were given by $A((E_m + B)/(1 - \exp((-B - E_m)/C)$, and β_{nF} and β_{nS} were given by $A(-B - E_m)/(1 - \exp((E_m + B)/C)$. The values of A, B and C used are indicated in Table 1.

Results

PKC inhibition prevents current up-regulation

Incorporating the non-selective protein kinase inhibitor H7 into the intracellular solution also containing GTP-γ-S and ATP, slowed and reduced the up-regulation of the persistent Na^+ current in $Na_V1.8$ null neurones in conventional whole-cell voltage-clamp (Baker *et al.* 2003). A high concentration of kinase inhibitor (200 μM) was necessary because of the simultaneous exposure of the neuronal contents to GTP-γ-S. Subsequent experiments are consistent with pre-exposure of WT neurones to 20 μM H7, for at least 30 min prior to recording, also attenuating current up-regulation (Fig. 1*A* and *B*). In order to define more rigorously whether protein kinase C (PKC) is involved in up-regulating persistent Na^+ current, the selective pseudosubstrate inhibitor PKC19–36 was incorporated into the intracellular solution along with GTP-γ-S and ATP. (In conventional whole-cell voltage-clamp recordings from $Na_V1.8$ null neurones, data are presented only from neurones in which a persistent Na^+ current could be perceived from near the start of recording.) The increase in current amplitude with GTP-γ-S and ATP only was close to 300% at 4–5 min in $Na_V1.8$ null neurones and this increase was abolished by adding the peptide inhibitor (Fig. 1*C*), providing evidence that at least one PKC isoform is involved ($P = 0.035$, 2-way repeated measures ANOVA, total $n = 10$, $n = 6$ without and with PKC19-36, respectively, data collected at 30 s intervals; $P < 0.01$ at 2 min and $P < 0.05$ at 4.5 min, one-tailed t test). The peptide inhibitor was present at a maximum concentration of 5 μM, although 500 nM also appeared effective. A 10 μM concentration of the inhibitor is reported to have a selective functional effect on PKC pathways modulating $Na_V1.8$ (Gold *et al.* 1998).

Activators of PKC, but not PKA, cause persistent current up-regulation

Confirmation of the involvement of PKC was obtained in conventional whole-cell patch-clamp experiments

in WT neurones, incorporating a selective activator of PKC in the internal solution. When the activator 1-oleoyl-2-acetyl-sn-glycerol (OAG, 25 μM) (Fig. 2) was present in addition to 3 mM ATP and 500 μM GDP, the persistent current amplitude and density measured during a voltage-clamp step to −40 mV (and more negative potentials) was up-regulated. This result was not found with GDP and ATP alone. In Fig. 2*A* can be seen TTX-r currents initially dominated by $Na_V1.8$, but after exposure to 25 μM internal OAG, the low threshold, persistent portion of the current was selectively up-regulated. The enhancement of the most negatively activating currents can be seen in the current-voltage ($I-V$) plots shown in *C*, appropriate for persistent Na^+ current up-regulation. Difference currents are clearly similar to persistent Na^+ currents, consistent with the up-regulation of persistent Na^+ current, with minimal changes in $Na_V1.8$ (Fig. 2*B* and *D*). In other WT neurones, the amplitude of the TTX-r current evoked at −40 mV was measured repeatedly over 5 min (Fig. 2*E*). Measurements from neurones that subsequently exhibited a persistent current and also those that did not were included in the analysis, because at these negative potentials and with internal GDP, it was initially difficult to tell whether a persistent current was present. The group of neurones exposed to OAG fell into two populations, either exhibiting up-regulation, or exhibiting no up-regulation ($n = 5$ and $n = 4$, respectively). These two groups differed significantly in their current densities ($P = 0.002$, two-way repeated measures ANOVA), a statistically significant difference being apparent after 30 s recording time, consistent with the presence of persistent current in only a fraction of neurones studied. I do not interpret the low initial current density (derived from the maximum inward current measured on the trace), or that

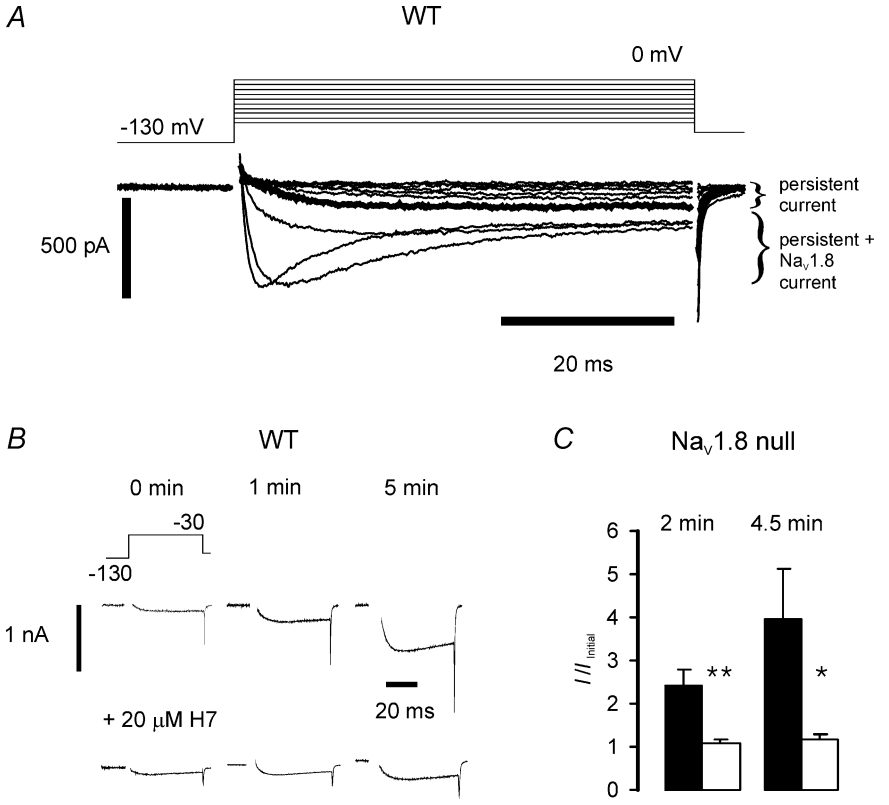

Figure 1. Kinase inhibition blocks the up-regulation of persistent Na^+ current
A, recording of TTX-r Na^+ currents, made immediately after attaining the whole-cell configuration in a wild-type (WT) neurone, which includes a low-threshold persistent portion. Heavy trace indicates current activated by a step to −30 mV. An interpretation of the currents evoked by depolarization (right) indicates that the current at −30 mV and more negative is largely persistent Na^+ current. *B*, Na^+ currents recorded in WT neurones in response to voltage-clamp steps to −30 mV. Dramatic up-regulation of the current amplitude followed the introduction of 500 μM GTP-γ-S to the neurone interior (by over 6 times within 5 min, same neurone as in *A*). After pre-exposure to 20 μM H7 in another neurone with a very similar initial current, up-regulation was near 150%. *C*, in $Na_V1.8$ null neurones, an intracellular solution containing GTP-γ-S and ATP (filled bars) gave rise to a substantial up-regulation of peak persistent current (I, measured at −10 mV or −20 mV, whichever was the larger) at 2 and 4.5 min ($n = 10$ and 8, respectively), in comparison to the initial current amplitude (I_0). The addition of 500 nM to 5 μM PKC19–36 to the intracellular solution with GTP-γ-S and ATP (open bars), blocked the up-regulation at 2 and 4.5 min ($n = 6$ and 4, respectively), consistent with a role for PKC. (*$P < 0.05$, **$P < 0.01$, one-tailed, unpaired t test.)

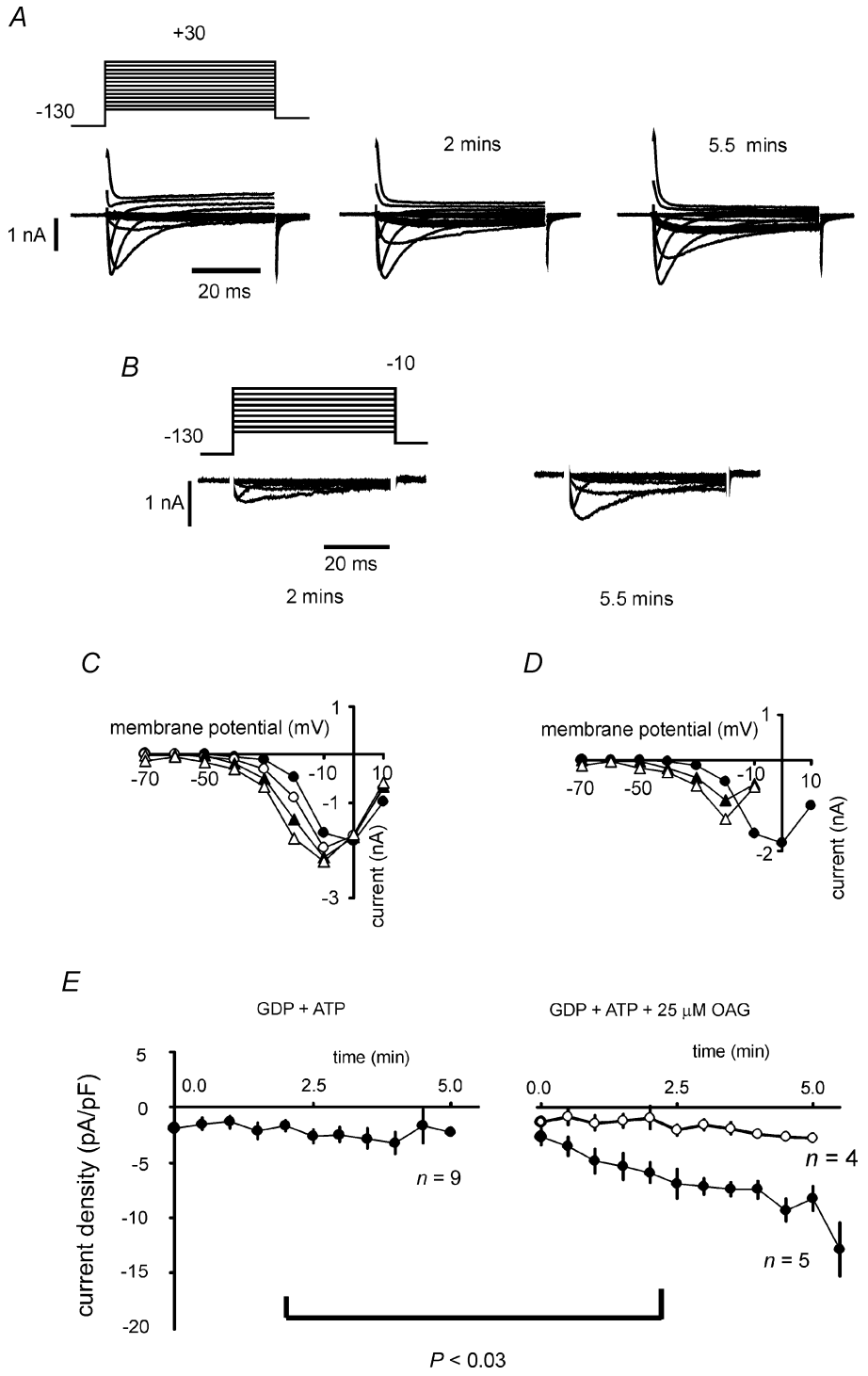

Figure 2. OAG in the pipette solution with GDP + ATP causes persistent Na^+ current up-regulation in WT neurones

A, families of TTX-r Na^+ currents evoked by the inset voltage-clamp protocol. At −40 mV, a potential more negative than the activation threshold for $Na_V1.8$, a persistent current was up-regulated over 5.5 min (dark traces). *B*, subtraction of initially recorded currents from those recorded later gives the component that was up-regulated, corresponding with persistent Na^+ current. *C*, *I*–*V* plots for peak Na^+ current at the start of recording (●), 2 min (○), 5.5 min (▲) and 7.5 min (△) into the voltage-clamp. *D*, *I*–*V* plots for initial peak Na^+ current (●), and for that component up-regulated at 5.5 min (▲) and 7.5 min (△). *E*, no up-regulation of current at −40 mV with GDP + ATP was apparent in 9 neurones (left hand panel), whereas 5 of 9 neurones with 25 μM internal OAG exhibited an up-regulation at −40 mV (right hand panel; $P < 0.03$, Fisher's exact test). In *E* those neurones showing no clear up-regulation in the right-hand panel (○) are presumably without functional persistent Na^+ current.

found throughout in the presence of internal GDP, as an indication of the presence of a low level of persistent current in all neurones; these small values almost certainly fall within baseline noise. This result was expected because expression of $Na_V1.9$-like immunoreactivity occurs in only a subpopulation of sensory neurones (e.g. Fang *et al.* 2002). The frequency with which up-regulated persistent current was recorded (in 5 of 9 neurones exposed to 25 μM OAG) was significantly different from that obtained with GDP alone ($P < 0.03$, Fisher's exact test; Fig. 2*E*).

Subsequently, using the perforated-patch technique to make recordings from both $Na_V1.8$ null and WT neurones, it was found that the membrane-permeant PKC activator phorbol 12-myristate 13-acetate (PMA) up-regulated the persistent current ($n = 5$), whereas 8-bromo-cyclic AMP (8Br-cAMP) and dibutyrylcyclic AMP (dbcAMP)(membrane permeant analogs of cAMP) did not ($n = 4$, when applied alone), even when tested in neurones also found to be responsive to PMA ($n = 2$; Fig. 3). The apparent changes in reversal potential during an experiment (e.g. Fig. 3*A*) may be partly caused by the progressive block of residual K^+ currents, associated with the diffusion of Cs^+ ions into the neurones. These data indicate that the up-regulation of persistent Na^+ current may specifically require activation of PKC. In response to exposure to 100 nM PMA, current up-regulation in $Na_V1.8$ null neurones occurred gradually, with a near 65% average increase in maximal amplitude over 5 min (Fig. 3*A* and *D*). There was little change in persistent current activation voltage dependence for the neurone in Fig. 3*A*, even when the current amplitude doubled between 5 and 25 min exposure (Fig. 3*B* and *C*). The less than 6 mV apparent hyperpolarizing shift in the half-maximal activation potential can possibly be explained by the effect of residual K^+ currents becoming proportionally less as the Na^+ current amplitude increased.

In contrast, in WT neurones intracellular OAG (cf. Fig. 2) or extracellular PMA (100 nM, $n = 4$; 1 μM, $n = 3$) had a small effect on the peak amplitude of the major TTX-r Na^+ current, $Na_V1.8$ (Fig. 4). There was a statistically significant increase in $Na_V1.8$ current amplitude (largest individual increase in maximal currents was 24%) with 100 nM PMA ($P = 0.004$, repeated measures 2-way ANOVA), between -10 and $+40$ mV ($P < 0.05$, *post hoc* Holm-Sidak test) although following exposure to 1 μM there was no significant change in current amplitude. Neither was there any obvious change in the voltage dependence of current recruitment after exposure to PMA. Superfusion of 8Br-cAMP gave a variable response ($n = 4$) from no effect to a substantial up-regulation (Fig. 4*E* and *F*) that was not reversed by washing. The gradual activation of $Na_V1.8$ with depolarization suggests that series-resistance errors across the perforated patches for presented data are likely to be small. That said, for Fig. 4*E* and *F*, taking the residual, uncompensated series resistance to be near to 1 MΩ for the during exposure data, the maximal series-resistance error at the peak would be expected to be close to 8 mV. However, the change in voltage errors between the control and exposure data is likely to be substantially less than this (probably less than 5 mV), because the voltage-clamped currents have similar amplitudes. Inadequacies in the quality of the voltage clamp caused by perforated-patch recording therefore cannot account for the pharmacological effect of PGE_2. This up-regulation is very similar to the effects reported by England *et al.* (1996) and Gold *et al.* (1996, 1998) and corresponds well with the effects of exposure to PGE_2 ($n = 6$; Fig. 5). PGE2 was without any acute effects on persistent Na^+ current (see below). One possibility is that the hyperalgesic effects of PGE_2 are mediated largely or wholly through the functional modulation of $Na_V1.8$ alone, explaining the dramatic effect of antisense against $Na_V1.8$ on PGE_2 induced hyperalgesia *in vivo* (Khasar *et al.* 1998).

Increased excitability accompanies an increase in persistent inward current

To address the question as to whether exposure to PMA can give rise to increases in excitability by a mechanism consistent with the up-regulation of persistent Na^+ current, perforated-patch recordings were made in voltage-clamp and current-clamp mode in the same neurone. In all perforated-patch experiments that included current-clamp recording, the extracellular solution was quasi-physiological, without TTX (Baker *et al.* 2003), and the intracellular solution contained $KMetSO_4$ (see Methods). In order to maximize the effects of the current on excitability, the neurones were routinely held at -80 or -90 mV by applying a holding current that was adjusted to maintain a steady membrane potential. Figure 6 includes recordings from an example neurone that show PMA-induced up-regulation of a low-threshold inward current, occurring simultaneously with a fall in the current threshold and a more negative voltage threshold for action potential firing. In six similar recordings, no increases in excitability were seen, and there was no perceptible up-regulation of a low-threshold inward current. This suggests that, at least in terms of changes in threshold measured from a negative holding potential, any effects on other transient Na^+ currents operating in the small diameter neurones by PKC activation are negligible. Furthermore, when using either perforated-patch or conventional whole-cell recording, and a pipette solution containing a near physiological $[K^+]$, it was common to observe a fall in excitability over time. This was attributed to an increase in low-threshold K^+ current possibly consistent with a gradually increasing intracellular $[K^+]$ in the neurone,

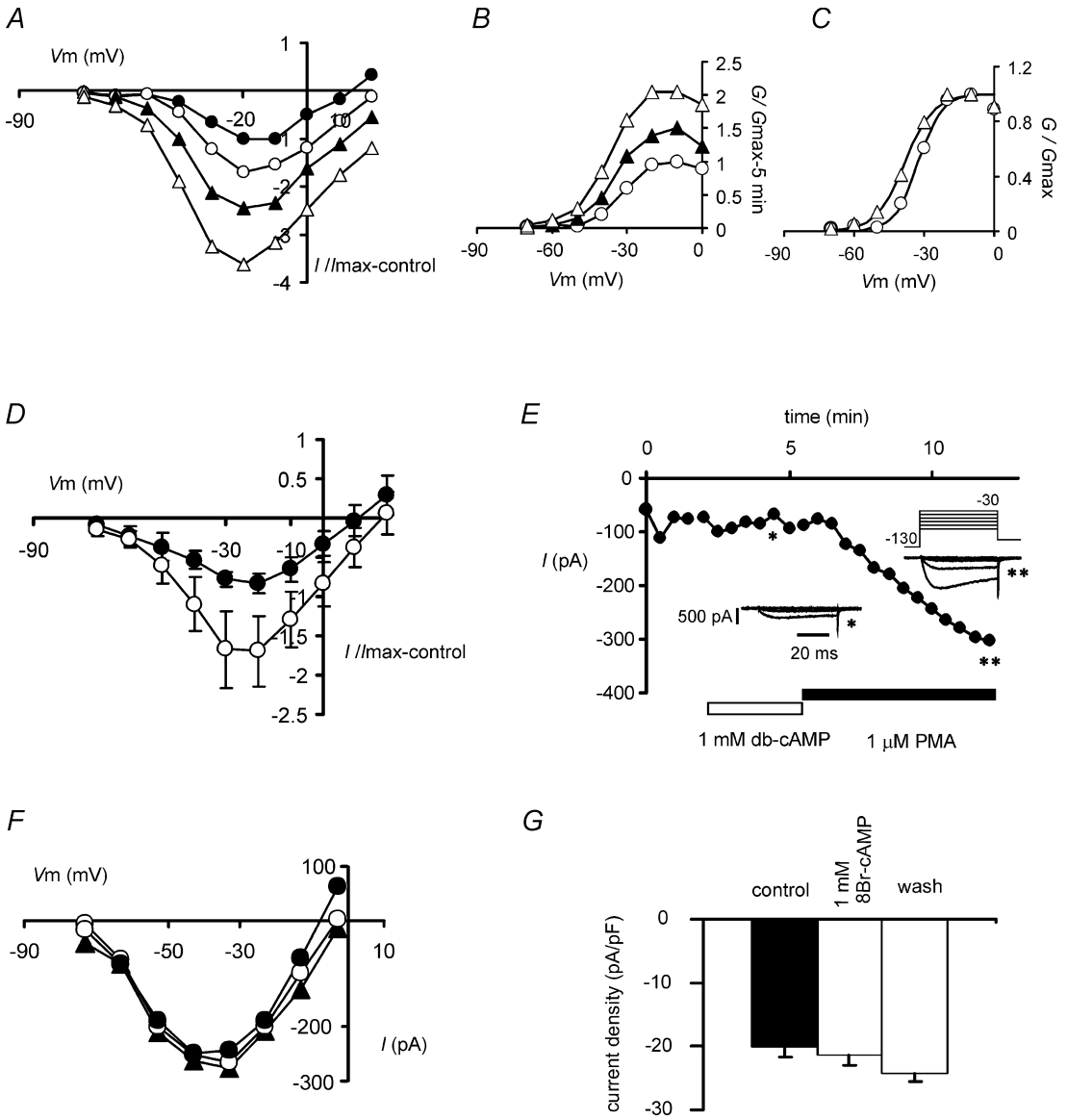

Figure 3. PMA up-regulates persistent Na^+ current, whereas membrane permeant activators of PKA do not

A, peak current–membrane potential relation for persistent Na^+ current in $Na_V1.8$ null neurone before (●) and during exposure to 100 μM PMA for up to 5 min (○), 15 min (▲) and 25 min (△). Any change in apparent reversal potential on exposure to PMA is caused by the up-regulation of persistent Na^+ current recorded against residual K^+ currents, and it does not represent a true change in reversal potential for Na^+. *B*, current amplitude values at 5, 15 and 25 min in *A* were converted to conductances, assuming E_{Na} to be +60 mV, normalized to the maximal conductance at 5 min, and plotted against membrane potential. The maximal conductance doubled between 5 and 25 min. *C*, normalized conductance values for 5 and 25 min, superimposed on Boltzmann relations, drawn with best-fit parameters, and giving half-maximal activation potentials of −32.6 and −38.3 mV, respectively. *D*, 100 μM PMA caused up-regulation of persistent Na^+ current in $Na_V1.8$ null neurones ($n = 5$) where data were obtained following an exposure lasting close to 5 min. Data normalized to maximal pre-exposure inward current for each neurone. *E*, exposure of a WT neurone to 1 mM db-cAMP does not up-regulate current amplitude at −40 mV, but 1 μM PMA causes an immediate and profound up-regulation ($n = 2$ where both agents were applied). *F*, *I*–*V* relation for persistent Na^+ current in an $Na_V1.8$ null neurone before, during and after (●, ○, △, respectively) exposure to 1 mM 8Br-cAMP for 2.5 min. Similar recordings with 500 μM 8Br-cAMP for up to 3 min were also without effect (total $n = 3$). *G*, peak TTX-r inward current densities in WT neurones, measured at −40 mV, before, following several minutes exposure to 1 mM 8Br-cAMP, and during wash ($n = 3$). The PKA activator does not appear to up-regulate persistent Na^+ current. All recordings made using perforated patches.

although this phenomenon was not studied in detail.

Extracellular ATP up-regulates persistent current

Because intracellular proteins are not dialysed when using the perforated-patch recording method, acute functional study of potential endogenous activators of G-protein pathways becomes possible, as the second messenger pathways should remain intact. Exposure to ATP (5–150 μM) caused acute up-regulation of the persistent current (measured in voltage-clamp in the presence of extracellular TTX; Fig. 7*A*–*C*) in both $Na_V1.8$ null neurones (4 responded of 6 exposed) and WT neurones (6 of 9 exposed appeared to have an up-regulated persistent current). Thus the overall response rate for neurones already generating the current was 67%. The up-regulation was apparent on a time scale of seconds to minutes. Currents measured to produce the plot in Fig. 7*C*, are shown in Fig. 7*D* and *E*, where it is apparent that although there is substantial amplitude up-regulation, the voltage-dependent kinetics of the current are unchanged,

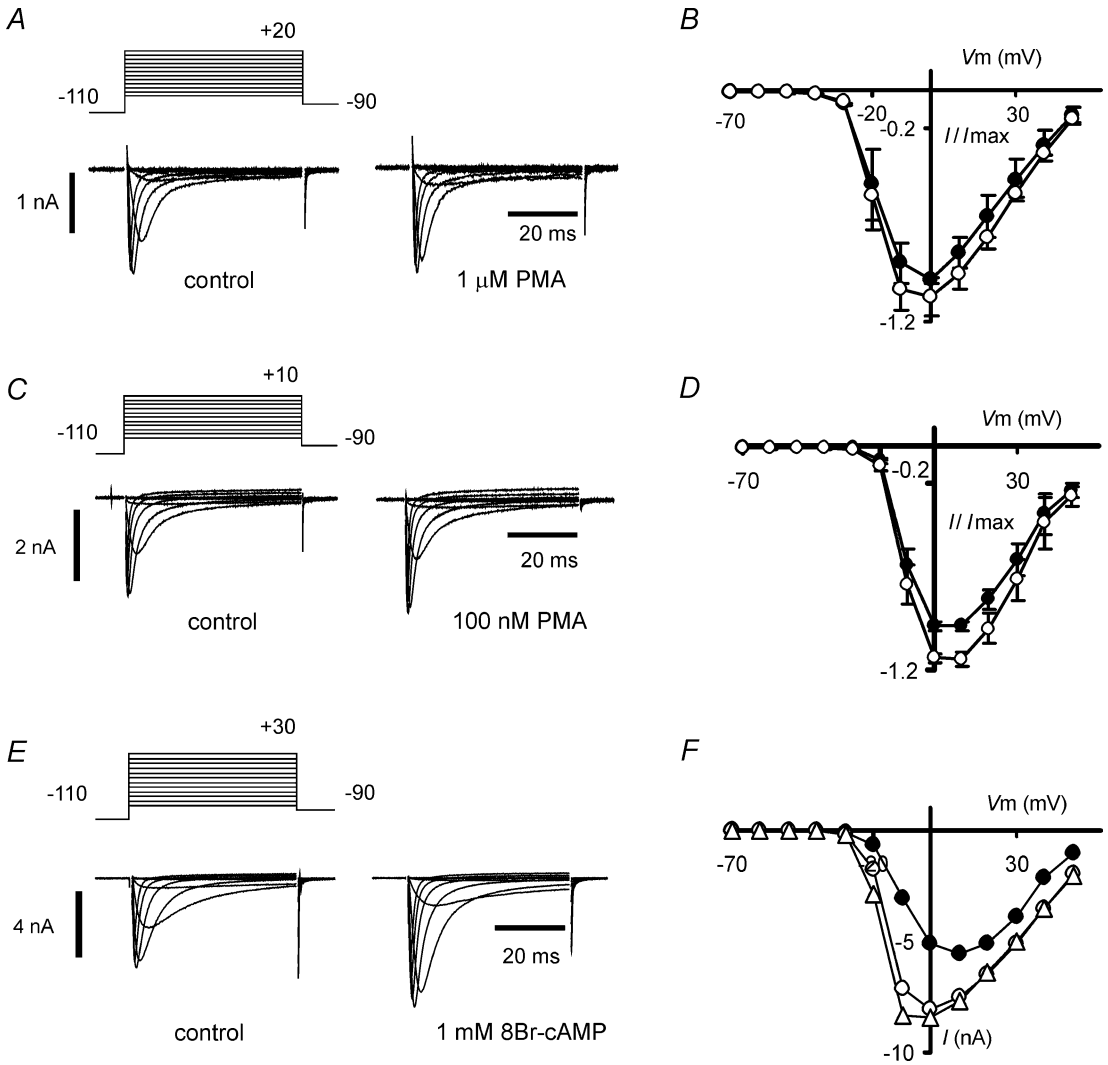

Figure 4. PMA exposure causes a small up-regulation in $Na_V1.8$ amplitude
A and *C*, representative Na^+ currents attributable to $Na_V1.8$ in WT neurones, and *B* and *D*, mean *I*–*V* relation (for 3 and 4 neurones, respectively) before and during superfusion of PMA at 1 μM (*A*) or 100 nM (*C*) over minutes (largest current amplitude values in both conditions before (●) and during (○) exposure, respectively). The values are normalized with respect to the maximal peak pre-exposure values. Larger increase in amplitude obtained with 100 nM PMA is a small but statistically significant change ($P = 0.004$, repeated measures, 2-way ANOVA), with the largest individual peak increase being close to 24%. *E* and *F*, superfusion of 1 mM 8Br-cAMP up-regulates $Na_V1.8$ in an example neurone. The peak current at 0 mV increased by 46% in minutes. *F*, *I*–*V* plots, for the same neurone in *E*, before (●), during exposure (○) and during washing (△). All recordings made using perforated patches and data points are not corrected for residual series-resistance errors.

consistent with minor or no changes in the voltage dependence of the persistent current, found also for PMA and GTP. In a WT neurone, the maximal current amplitude was measured at −40 mV (or more negative), potentials at which little or no contribution of $Na_V1.8$ would be expected. Based on cumulative concentration-response experiments, the effect of ATP exhibited an average apparent K_d near 13 μM. The largest up-regulation on exposure to a particular concentration of ATP was expressed as a fraction of that predicted to be the maximum possible after up-regulation, by fitting each individual data set by a Langmuir isotherm, and thus only data sets incorporating at least two ATP test concentrations could be included in the analysis (Fig. 7*B*). This analysis may underestimate the true potency of ATP for two reasons. Because these data were obtained by generating a cumulative concentration response to ATP, the up-regulation at the lowest concentrations tested may not have been fully complete before a higher concentration was applied (potentially reducing the apparent potency of low concentrations), and any tendency to spontaneous up-regulation during recording might increase the amount of apparent up-regulation caused by the higher concentrations, potentially skewing the estimate of K_d to a higher value.

PGE_2 is known to up-regulate $Na_V1.8$ (e.g. Gold *et al.* 1996, 1998), on a time scale of seconds to minutes and this mechanism has been proposed to participate in hyperalgesia following inflammation. The actions of PGE_2 include effects on the amplitude and voltage dependence of $Na_V1.8$ and are most similar to the effects of directly activating PKA. The action of PGE_2 is mimicked by

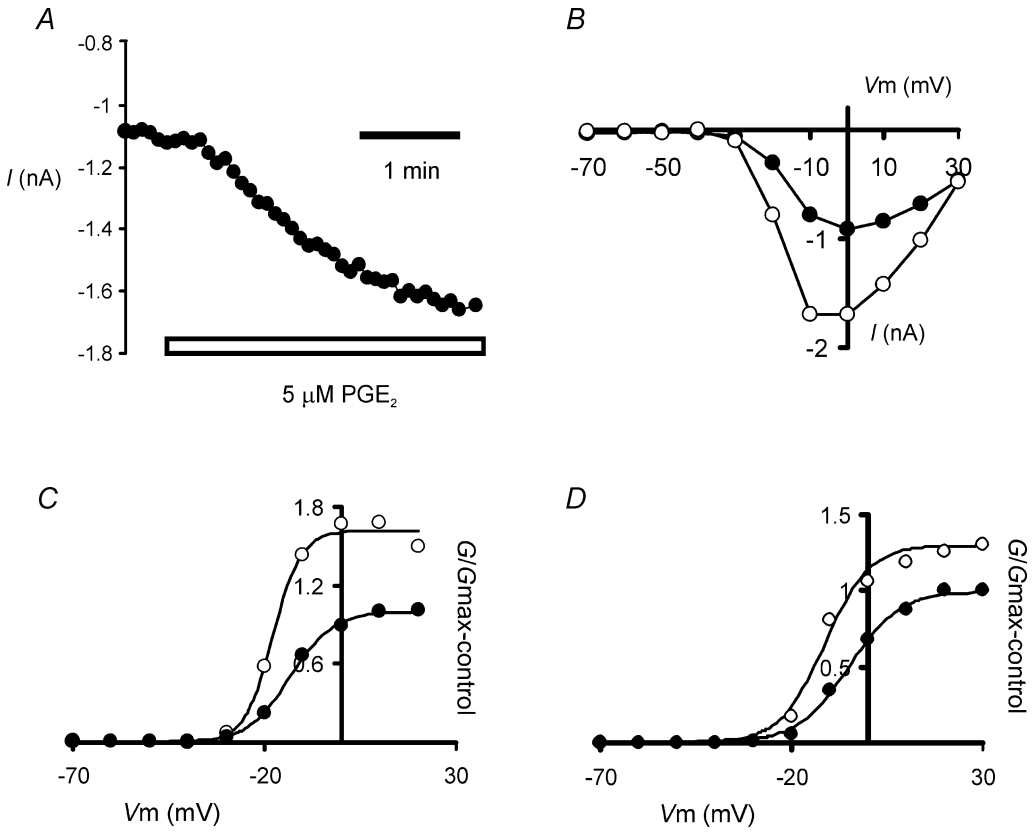

Figure 5. PGE_2 exposure and activation of PKA acutely up-regulates $Na_V1.8$
A, superfusion of 5 μM PGE_2 caused an up-regulation of $Na_V1.8$ amplitude, recorded at +10 mV. Similar results were obtained in 6 neurones. *B*, peak current-voltage relations for the same neurone in *A*, recorded before (●) and after (○) exposure to PGE_2 (i.e. immediately before and after making the recordings for *A*). *C*, plot of normalized peak conductance values against membrane potential, derived from the current values in *B*, before (●) and after (○) exposure to PGE_2. Smooth curves are Boltzmann relations with maximal amplitudes of 1 and 1.62, and half-maximal activation potentials of −13.34 and −17.82 mV before and after exposure to PGE_2, respectively. Conductances were derived assuming E_{Na} to be +60 mV. *D*, normalized peak conductance *versus* membrane potential plot, before and during exposure to 8Br-cAMP (1 mM); same cell as in Fig. 4*E* and *F*. Smooth curves are Boltzmann relations with maximal amplitudes of 1 and 1.3 and half-maximal activation potentials of −4.98 and −11.32 mV before and after exposure to 8Br-cAMP. E_{Na} was assumed to be +62 mV. Data points were not corrected for residual series-resistance errors. All recordings made using perforated patches.

activators of PKA and blocked by PKA inhibition (England *et al.* 1996; Gold *et al.* 1998). PGE_2 exposure is also reported to have a chronic up-regulatory effect on the persistent Na^+ current amplitude, when neurones are incubated in the presence of 10 μM PGE_2 for 1 h (Rush & Waxman, 2004), through an unknown mechanism involving $G_{i/o}$. The effects of micromolar range PGE_2 were therefore tested on persistent Na^+ current, and no clear effects of any kind were seen in response to acute exposure over 5 min ($n = 12$).

Numerical simulation qualitatively reproduces excitability changes seen with persistent current up-regulation

Example real and simulated TTX-r Na^+ currents recorded in voltage-clamp are shown in Fig. 8*A* and *C* ($Na_V1.8$ and persistent Na^+ current, respectively). The peak-current-voltage relations for the two types of TTX-r current are shown in Fig. 8*B* and *D*. Simulated $Na_V1.8$ current activates around −30 mV, whereas the persistent Na^+ current activates close to −60 to −65 mV (cf. Baker & Wood, 2001). In Fig. 8*E* and *F* are shown the simulated activation and h_∞ curves for $Na_V1.8$ and persistent Na^+ current. Ultra-slow inactivation gating of the persistent Na^+ current (e.g. Cummins *et al.* 1999; Herzog *et al.* 2001) was not included in the simulation, and this can be justified because the aim of the simulation was to help test the hypothesis that up-regulation of persistent Na^+ current might be able to replicate the change in firing properties seen in current-clamped neurones, and also whether its up-regulation could cause spontaneous activity. Cleary ultra-slow inactivation would be expected to play a role in curtailing firing or any increase in excitability occurring as a result of persistent Na^+ current up-regulation.

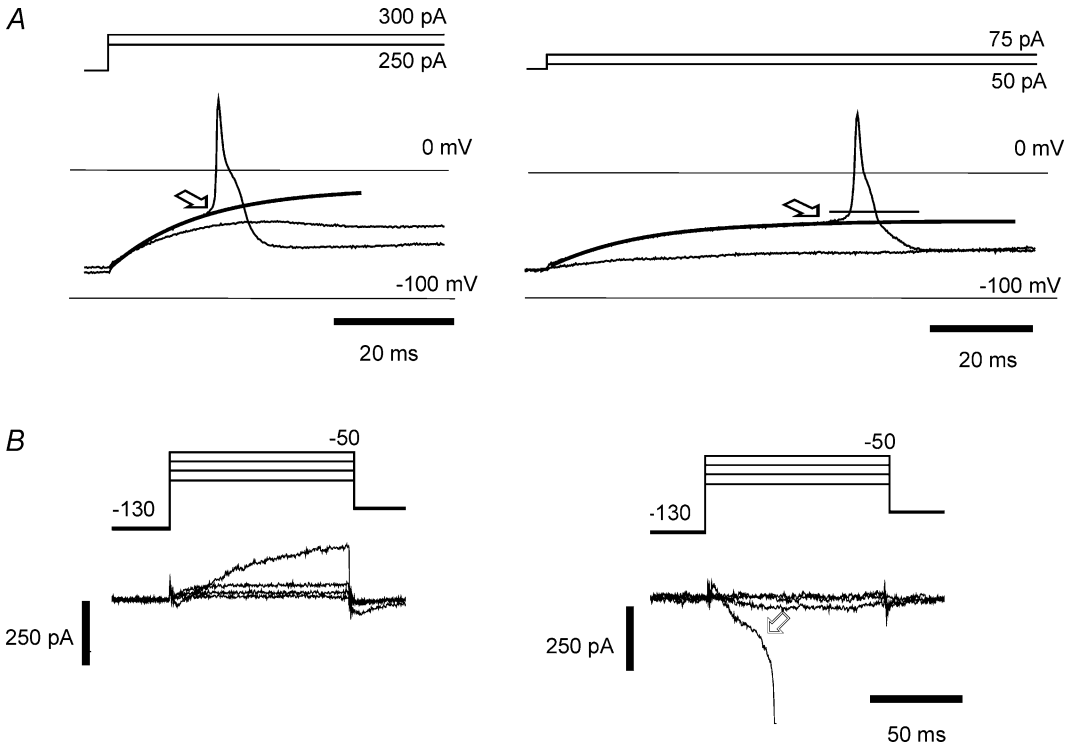

Figure 6. Negative shift in voltage threshold and the simultaneous up-regulation of a low-threshold inward current

A, current-clamp (perforated-patch) recordings in control solution and at 10 min following exposure to 1 μM external PMA in a WT neurone (left and right hand panels, respectively). Neurone held near −80 mV, before step depolarizations. Smooth lines are exponentials drawn according to best-fit parameters, whose trajectory approximates the passive membrane response to depolarization. An increase in excitability results in a negative shift in voltage threshold, from −43 to −52 mV (indicated by arrows), and an increase in the latency of the action potential generated by a near threshold depolarization. The estimated voltage-threshold in the control recording is indicated on the action potential in the right hand panel as a short line. *B*, voltage-clamp recordings from the same neurone as in *A*. Under control conditions, no low-threshold inward current was observed (left-hand panel). After exposure to PMA, a persistent inward current contributes at negative potentials (change in current is plotted, right-hand panel). With a voltage-clamp step to −50 mV, inadequacies in the voltage-clamp prevented control of the Na^+ current and the current became regenerative (arrow).

Action potentials and associated action currents in a simulated neurone normally held at −90 mV are shown in Fig. 9*A*. The neurone was held at −90 mV by passing a continuous hyperpolarizing current, clearly visible at the start and end of the current traces. The results of the simulation replicated experimental findings quite well (Baker *et al.* 2003). Up-regulation of persistent Na^+ current is associated with a fall in current threshold, the prolongation of subthreshold depolarizations beyond the offset of an applied current, and an increase in the latency of an action potential evoked by a just-suprathreshold depolarization. Up-regulation of the current is also associated with repetitive firing at membrane potentials substantially more negative than the voltage threshold for action potential induction before current up-regulation (Fig. 9*B*). This present model was also modified to produce sustained firing in a neurone not receiving external stimulation. Before adding the persistent Na^+ current, increasing the neurone input resistance from the initial 200 MΩ to 2 GΩ gave a membrane potential of −58.4 mV, without the application of any polarizing current, and this was taken as the resting state. If the persistent Na^+ current only was subsequently included, the membrane potential was found to stabilize at a new, low value within the range of persistent current activation-inactivation overlap, and sustained firing was not seen. However, with the simultaneous addition of a hyperpolarizing 'pump-current', sustained firing occurred (Fig. 9*C*), providing at least a qualitative confirmation that persistent Na^+ current may be able to drive spontaneous activity in a living neurone, but perhaps only where its tendency to depolarize is countered by the Na^+ pump.

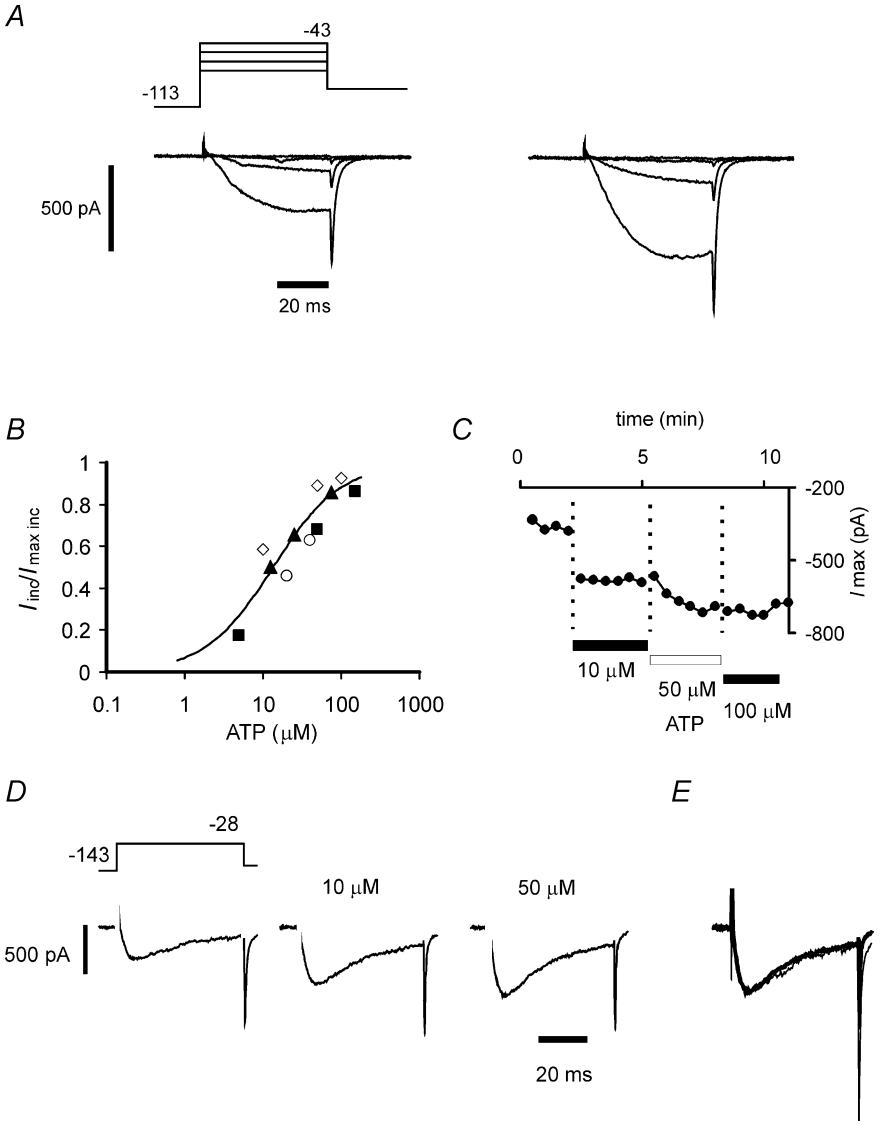

Figure 7. Persistent Na^+ current is up-regulated by exposure to external ATP
A, TTX-r inward currents recorded at negative potentials in a WT neurone were up-regulated within a minute following exposure to a bolus of ATP introduced into the recording chamber (final concentration 50 μM). Left hand panel, and right hand panel before and after ATP introduction, respectively. *B*, increment in current amplitude (I_{inc}) on exposure to ATP (continuous superfusion) plotted as a fraction of maximum increase possible ($I_{max\ inc}$) in each neurone. The maximum increase for each neurone was found by fitting an isotherm to the raw amplitude values. Each symbol type represents an individual neurone. ○, ▲, △ indicate peak current values from $Na_V1.8$ null neurones and, ■ from WT (in the latter the current amplitude was measured at −40 mV). Smooth curve is a Langmuir isotherm drawn according to parameters providing the best-fit to all data points, with an apparent $K_d = 13$ μM. *C*, example increases in Na^+ current amplitude on exposure to increasing concentrations of ATP in an $Na_V1.8$ null neurone (exposure time indicated by the bars beneath the data points). *D*, increase in Na^+ current amplitude measured at −28 mV, before and after exposure to 10 and 50 μM ATP in an $Na_V1.8$ null neurone (same as that in panel *C*). *E*, scaled version of control current in *D* (thin line), superimposed on current recorded in the presence of 50 μM ATP (thick line). No obvious changes in current kinetics occurred as the current amplitude increased, consistent with unchanged gating voltage dependence.

Discussion

The TTX-r Na^+ channels present in primary afferents, $Na_V1.8$ and $Na_V1.9$, are both found in nociceptors (e.g. Akopian *et al.* 1999; Fjell *et al.* 2000; Fang *et al.* 2002). Functional evidence places TTX-r Na^+ channels at unmyelinated nerve endings, where they are involved in action potential generation and propagation, indicative of a role certainly for $Na_V1.8$ (Brock *et al.* 1998; Strassman & Raymond, 1999). Immunohistochemical evidence indicates the expression of $Na_V1.9$ in the corneal leash fibres (Black & Waxman, 2002). One shared functional characteristic of the TTX-r Na^+ channels in primary afferents is that they can be profoundly modulated by second messenger pathways, to an extent dramatic enough to be consistent with a contribution to inflammatory pain (e.g. Khasar *et al.* 1998). The mechanism by which membrane conductance is increased remains unresolved in both cases, but the data presented here show that PKC probably plays a crucial role in the up-regulation of persistent Na^+ current, attributed to $Na_V1.9$. Protein kinase activation, especially PKA, underlies the up-regulation of $Na_V1.8$ (England *et al.* 1996; Gold *et al.* 1998; Fitzgerald *et al.* 1999). Gold *et al.* (1998) report that phorbol esters (including PMA) cause up-regulation of $Na_V1.8$, and that PKC activation is likely to contribute to the PGE_2-induced modification of $Na_V1.8$ Na^+ currents, although the up-regulation of $Na_V1.8$ by exposure to PGE_2 is most similar to that brought about by PKA activation. While PKC may indeed contribute to the PGE_2-induced up-regulation of $Na_V1.8$, the effects of PMA reported here are small. The present experiments suggest that PGE_2 is without acute effects on persistent Na^+ current, and this seems consistent with the lack of effect of PKA activation on the current.

Baker *et al.* (2003) reported that between 1 in 3 and 1 in 6 neurones exhibited persistent Na^+ current, in voltage-clamp and current-clamp recordings, respectively. The currents are probably easier to spot in voltage clamp with the K^+ channels blocked. The OAG experiments reported here found something like 1 in 2, quite similar to that expected from the immunocytochemical evidence (Fang *et al.* 2002). The apparent small discrepancy between the present voltage-clamp recordings and previous ones might indicate that internal application of OAG is very effective at up-regulating the current. A number of possibilities might explain the functional up-regulation of persistent Na^+ current. These include an obligatory

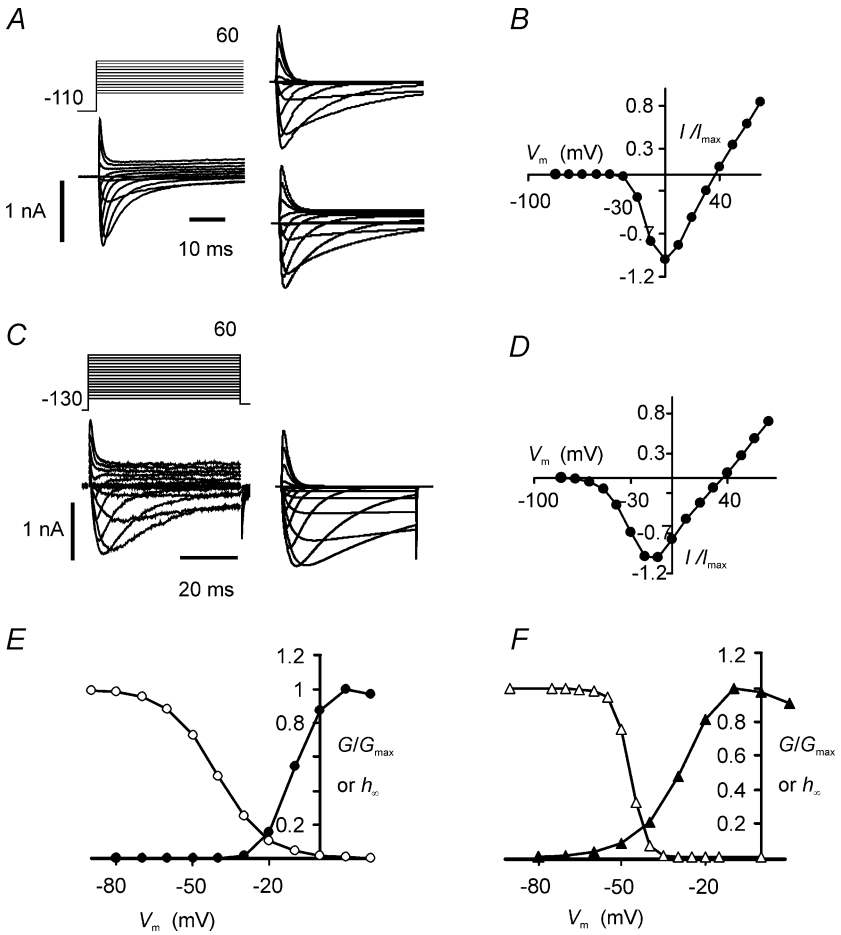

Figure 8. Characteristics of Na^+ currents incorporated into numerical simulation
A, left panel, typical example $Na_V1.8$ currents recorded in the presence of TTX and simulated currents (right panel). Simulated Na^+ currents without and with residual fast K^+ current (upper and lower family of voltage-clamp traces, respectively). *B*, the corresponding peak *I*–*V* plot for simulated currents (without K^+currents) using a one-third physiological Na^+ gradient. *C*, example persistent Na^+ currents recorded in $Na_V1.8$ null in the presence of TTX, and simulated currents. Real currents show some residual delayed rectification that remains following exposure to K^+ channel blockers. *D*, corresponding peak *I*–*V* plot for simulated currents. *E*, G/G_{max} (activation, ●) and h_∞ (inactivation, ○) curve for simulated $Na_V1.8$. The values of h_∞ were calculated directly from rate constants, whereas the activation curve was obtained by measuring the peak currents generated in a voltage-clamp protocol with a negative holding potential, and converting them to conductances. *F*, activation and inactivation curves for persistent Na^+ current, G/G_{max} (●) and h_∞ (▲). The effect of inactivation rate on peak conductance can be observed at potentials more positive than −10 mV. The effects of ultra-slow inactivation on persistent Na^+ current were not included in the simulation.

phosphorylation of the channels by PKC before they can conduct, the possibility that PKC is involved in facilitating channel trafficking to the membrane, or that phosphorylation by PKC increases the single channel conductance of already operable channels (for example by favouring a larger conductance state over another smaller one), or some combination.

Evidence exists implicating at least one isoform of PKC in the induction of painful states. Bradykinin sensitizes a heat-activated current in cultured DRG neurones, through a PKCε-mediated mechanism. The PKCε isoform exhibits membrane translocation in response to activation of the second messenger pathway (Cesare & McNaughton, 1996; Cesare *et al.* 1999). PKCε inhibition is reported to reduce (up to 50%) an enhancement of TTX-r Na^+ current amplitude measured at −15 mV (in this case $Na_V1.8$) on exposure of cultured neurones to adrenaline (Khasar *et al.* 1999*a*,*b*) although it seems that the major modifier of the current in response to adrenaline exposure is PKA (Khasar *et al.* 1999*b*). The form of the enhancement appears very similar to that induced by PGE_2 (e.g. England *et al.* 1996; Gold *et al.* 1998) with an increase in the steepness of activation voltage dependence, leading to enhanced repetitiousness in current-clamp experiments.

Up-regulation of persistent Na^+ current and the consequences for nociceptor excitability

The function of the persistent Na^+ current has been controversial, because it begins to activate over a negative range of membrane potentials in sensory neurones (initially thought to be near −70 mV, but now reported to be between −50 and −70 mV; see Dib-Hajj *et al.* 2002; Rugiero *et al.* 2003; Baker *et al.* 2003) and with a negative steady-state inactivation voltage dependence, leading to the suggestion that the current is largely inactivated at the resting potential and may therefore be without function. Rugiero *et al.* (2003) have provided evidence that this is not the case in myenteric neurones, when recordings are made without internal F^-. These authors recorded persistent Na^+ current beginning to activate near −50 mV without intracellular F^-, but at −65 mV with intracellular

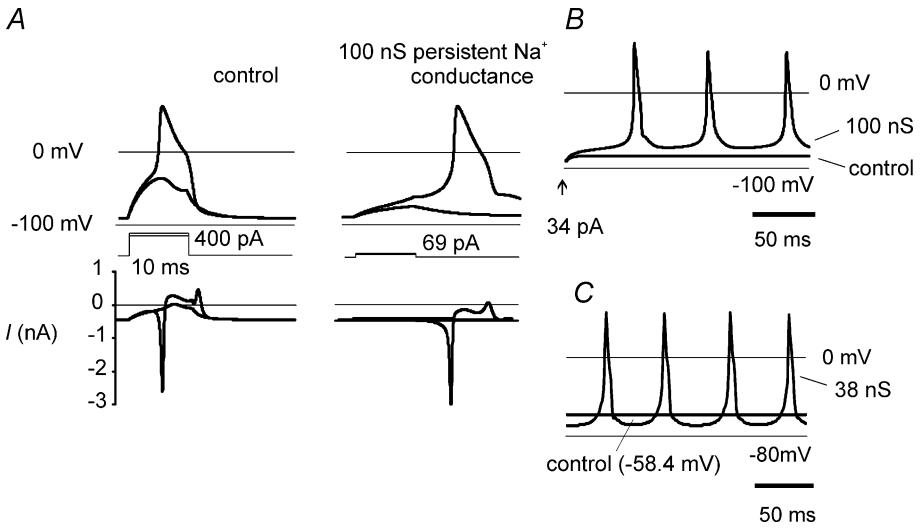

Figure 9. Simulated neurone exhibits characteristic changes in firing properties on up-regulation of persistent Na^+ current

A, just sub- and just supra-threshold responses from a control simulated neurone, lacking persistent Na^+ current, being held at −90 mV (left hand panel). The action potential was evoked within the 10 ms stimulus duration. Just sub- and just supra-threshold rectangular, applied depolarizing currents, lasting 10 ms are shown inset, where the larger current represents a change in holding current of 400 pA. Beneath are plotted the total transmembrane currents for both responses (bottom of left hand panel). The supra-threshold response includes a regenerative Na^+ current. Addition of persistent Na^+ current with a maximal conductance of 100 nS dramatically reduced the applied current threshold and the action potential was elicited with a more negative voltage threshold (right hand panel). The regenerative inward current (and the action potential upswing) occurs after the applied depolarizing current has ceased (bottom of right-hand panel). *B*, up-regulation of persistent Na^+ current gives rise to repetitive firing in response to a prolonged, just-supratheshold depolarization, a response not seen in the control neurone lacking the conductance. Initially the membrane potential was held at −90 mV by polarizing current and depolarization was brought about by a 34 pA change in holding current. The most negative interspike potential was close to −70 mV. *C*, simulation of a neurone with an input resistance of 2 GΩ, giving a resting membrane potential (without persistent Na^+ conductance) of −58.4 mV (control). Addition of persistent Na^+ conductance with a maximal value of 38 nS and with the simultaneous addition of a steady 60.5 pA hyperpolarizing 'pump current' produces a train of action potentials.

F^-, suggesting that the very negative activation voltage dependence originally reported for DRG neurones may be unphysiological, and related to the presence of a high internal [F^-] (cf. Cummins *et al.* 1999; Dib-Hajj *et al.* 2002). Rugiero *et al.* (2003) also defined the voltage dependence of the normal and ultra-slow inactivation of persistent Na^+ current in the absence of F^-, and their analysis indicates that steady-state inward currents are expected in myenteric neurones at −50 mV. In other experiments without intracellular F^-, the steady-state component of the up-regulated current has been found to be substantial enough to depolarize DRG neurones by more than 10 mV starting from a resting potential near −60 mV (Baker *et al.* 2003). While moderate depolarization can increase excitability and generate action potentials, prolonged and strong depolarization enhances the resting inactivation of transient Na^+ channels, leading to another speculation that the role of persistent Na^+ current is to reduce excitability at nerve endings by inactivating transient Na^+ channels (Herzog *et al.* 2001). However, persistent Na^+ channels seem to exist in operable and initially inoperable pools, or more than one functional state, allowing for receptor activation-dependent up-regulation of the current, and the possibility that in the quiescent state, the channels are not operating to depolarize the membrane.

The real resting potentials of C-fibres remain unknown, but strong indirect evidence from the velocity recovery cycles of C-fibres in human skin (Bostock *et al.* 2003) shows that at rest few voltage-dependent K^+ channels can be open, because activity-dependent increases in supernormality (attributable to electrogenic hyperpolarization) are not accompanied by a change in the membrane time constant. The resting potential of human C-fibres thus cannot be low and may be remarkably dependent on active pump current, rather than a resting K^+ conductance. On this basis, the normal membrane potential estimates (around −60 mV) made in the soma (e.g. Wang *et al.* 1994) may either be representative or perhaps less negative than the true membrane potential in C-fibres and persistent Na^+ channels might be able to elicit increases in excitability and depolarize the membrane potential in a manner dependent on the activation of G-protein coupled receptors. However, a different and apparently contradictory insight into the resting potentials of unmyelinated nerve endings is provided by the experiments of Carr *et al.* (2002) on the behaviour of Na^+ channels in cold-sensitive and polymodal endings in the guinea pig cornea. All endings appeared to be chronically depolarized, with substantial resting inactivation of transient Na^+ current, that could be reversed by passing hyperpolarizing current from an electrode. In fact, the inward Na^+ current (in polymodal receptors being largely but not exclusively TTX-r) could be approximately doubled in amplitude by the application of polarizing current, leading the authors to suggest that the nerve terminal membrane potentials were somewhere near −30 mV or even more positive. In cold-sensitive fibres this depolarized condition could be partly attributed to the chronic activation of cold-gated ion channels (Carr *et al.* 2003). If this estimate of nerve terminal resting potential is close to the physiological value, it is difficult to envisage a function for persistent Na^+ channels in terminals already operating at such depolarized potentials. However, as $Na_V1.9$-like immunoreactivity has a rather widespread expression pattern within the final axonal arborization (see Black & Waxman, 2002), then it might function to regulate excitability within a region of more negative membrane potential several microns or more from the transduction site.

ATP receptors

ATP is an algogenic agent that is released from damaged tissue (e.g. Burnstock, 2001), and cell damage can excite nociceptors *in vitro*, in a manner reproduced by exposure to ATP alone (e.g. Cook & McCleskey, 2002). P2X receptors (ATP-gated ion channels) are expressed by a subset of sensory neurones, and $P2X_3$ receptors have been implicated in nociception (Chen *et al.* 1995; Souslova *et al.* 2000). Activation of $P2X_3$ receptors in cultured neurones generates large, transient inward currents, that desensitize (e.g. Lewis *et al.* 1995; Ueno *et al.* 1999; Souslova *et al.* 2000). These receptors are implicated in an excitation of cultured neurones following exposure to ATP, and, in current-clamp, give rise to a period of firing lasting about a second (Molliver *et al.* 2002). Activation of P2Y receptors, on the other hand, give rise to a more prolonged period of action potential firing in cultured neurones (Molliver *et al.* 2002) through an unknown mechanism, and these receptors activate G-protein pathways probably acting on more than one final target (e.g. Molliver *et al.* 2002; Huang *et al.* 2003). The up-regulation of persistent Na^+ current on exposure to ATP, where the up-regulated amplitude is maintained over minutes in the presence of the agonist, provides a mechanism by which sensory neurones could be made hyperexcitable and this may explain the prolonged period of action potential firing on exposure to ATP.

The P2Y receptors expressed in sensory neurones include $P2Y_1$, $P2Y_2$ and $P2Y_4$, although the levels of $P2Y_4$ mRNA are low (Nakamura & Strittmatter, 1996; Tominaga *et al.* 2001; Mollivier *et al.* 2002; Sanada *et al.* 2002; Huang *et al.* 2003; Moriyama *et al.* 2003). There is evidence that both $P2Y_1$ and $P2Y_2$ receptor activation can temperature sensitize TRPV1-mediated currents, the former via a PKC-coupled pathway (Tominaga *et al.* 2001) although it seems that $P2Y_2$ is the more important receptor *in vivo*

(Moriyama *et al.* 2003). Evidence suggests that $P2Y_2$ is widely expressed by sensory neurones (e.g. Mollivier *et al.* 2002; Huang *et al.* 2003), whereas $P2Y_1$ may be primarily expressed in large, low-threshold mechanosensory neurones (Nakamura & Strittmatter, 1996). Furthermore, the P2Y agonist UTP has been found to activate functionally identified cutaneous afferents in a skin nerve preparation, almost all of which also responded to capsaicin (Stucky *et al.* 2004), indicating that they are nociceptive. As UTP acts relatively selectively on $P2Y_2$ and $P2Y_4$ receptor subtypes (Ralevic & Burnstock, 1998) these results may indicate the presence of these receptors in nociceptive endings, activation of which could stimulate PKC via a $G_{q/11}$ protein pathway. G protein pathway-coupled ATP receptors might therefore alter neuronal excitability, at least in part, through functionally up-regulating persistent Na^+ current.

References

Akopian AN, Souslova V, England S, Okuse K, Ogata N, Ure J, Smith A, Kerr BJ, McMahon SB, Boyce S, Hill R, Stanfa LC, Dickenson AH & Wood JN (1999). The tetrodotoxin-resistant sodium channel SNS has a specialized function in pain pathways. *Nat Neurosci* **2**, 541–548.

Baker MD & Bostock H (1997). Low-threshold, persistent sodium current in rat large dorsal root ganglion neurons in culture. *J Neurophysiol* **77**, 1503–1513.

Baker MD, Chandra SY, Ding Y, Waxman SG & Wood JN (2003). GTP-induced tetrodotoxin-resistant Na^+ current regulates excitability in mouse and rat small diameter sensory neurones. *J Physiol* **548**, 373–382.

Baker MD & Wood JN (2001). Involvement of Na^+ channels in pain pathways. *Trends Pharmacol Sci* **22**, 27–31.

Black JA & Waxman SG (2002). Molecular identities of two tetrodotoxin-resistant sodium channels in corneal axons. *Exp Eye Res* **75**, 193–199.

Bostock H, Baker M & Reid G (1991). Changes in excitability of human motor axons underlying post-ischaemic fasciculations: evidence for two stable states. *J Physiol* **441**, 537–557.

Bostock H, Campero M, Serra J & Ochoa J (2003). Velocity recovery cycles of C fibres innervating human skin. *J Physiol* **553**, 649–663.

Bostock H & Rothwell JC (1997). Latent addition in motor and sensory fibres of human peripheral nerve. *J Physiol* **498**, 277–294.

Brock JA, McLachlan EM & Belmonte C (1998). Tetrodotoxin-resistant impulses in single nociceptor nerve terminals in guinea-pig cornea. *J Physiol* **512**, 211–217.

Burnstock G (2001). Purine-mediated signalling in pain and visceral perception. *Trends Pharmacol Sci* **22**, 182–188.

Carr RW, Pianova S & Brock JA (2002). The effects of polarizing current on nerve terminal impulses recorded from polymodal and cold receptors in the guinea-pig cornea. *J General Physiol* **120**, 395–405.

Carr RW, Pianova S, Fernandez J, Fallon JB, Belmonte C & Brock JA (2003). Effects of heating and cooling on nerve terminal impulses recorded from cold-sensitive receptors in the guinea-pig cornea. *J General Physiol* **121**, 427–439.

Cesare P, Dekker LV, Sardini A, Parker PJ & McNaughton PA (1999). Specific involvement of PKC-epsilon in sensitization of the neuronal response to painful heat. *Neuron* **23**, 617–624.

Cesare P & McNaughton PA (1996). A novel heat-activated current in nociceptive neurons and its sensitization by bradykinin. *Proc Natl Acad Sci U S A* **93**, 15435–15439.

Chen CC, Akopian AN, Sivilotti L, Colquhoun D, Burnstock G & Wood JN (1995). A P2X purinoceptor expressed by a subset of sensory neurons. *Nature* **377**, 428–431.

Cook SP & McCleskey EW (2002). Cell damage excites nociceptors through release of cytosolic ATP. *Pain* **95**, 41–47.

Cummins TR, Dib-Hajj SD, Black JA, Akopian AN, Wood JN & Waxman SG (1999). A novel persistent tetrodotoxin-resistant sodium current in SNS-null and wild-type small primary sensory neurons. *J Neurosci* **19**, RC43.

Dib-Hajj S, Black JA, Cummins TR & Waxman SG (2002). NaN/Na_V1.9: a sodium channel with unique properties. *Trends Neurosci* **25**, 253–259.

England S, Bevan S & Docherty RJ (1996). PGE_2 modulates the tetrodotoxin-resistant sodium current in neonatal rat dorsal root ganglion neurones via the cyclic AMP-protein kinase A cascade. *J Physiol* **495**, 429–440.

Fang X, Djouhri L, Black JA, Dib-Hajj SD, Waxman SG & Lawson SN (2002). The presence and role of the tetrodotoxin-resistant sodium channel Na_v1.9 (NaN) in nociceptive primary afferent neurons. *J Neurosci* **22**, 7425–7433.

Fitzgerald EM, Okuse K, Wood JN, Dolphin AC & Moss SJ (1999). cAMP-dependent phosphorylation of the tetrodotoxin-resistant voltage-dependent sodium channel SNS. *J Physiol* **516**, 433–446.

Fjell J, Hjelmstrom P, Hormuzdiar W, Milenkovic M, Aglieco F, Tyrrell L, Dib-Hajj S, Waxman SG & Black JA (2000). Localization of the tetrodotoxin-resistant sodium channel NaN in nociceptors. *Neuroreport* **11**, 199–202.

Gold MS, Levine JD & Correa AM (1998). Modulation of TTX-R INa by PKC and PKA and their role in PGE_2-induced sensitization of rat sensory neurons in vitro. *J Neurosci* **18**, 10345–10355.

Gold MS, Reichling DB, Shuster MJ & Levine JD (1996). Hyperalgesic agents increase a tetrodotoxin-resistant Na^+ current in nociceptors. *Proc Natl Acad Sci U S A* **93**, 1108–1112.

Herzog RI, Cummins TR & Waxman SG (2001). Persistent TTX-resistant Na^+ current affects resting potential and response to depolarization in simulated spinal sensory neurons. *J Neurophysiol* **86**, 1351–1364.

Hodgkin AL & Huxley AF (1952). A quantitative description of membrane current and its application to conduction and excitation in nerve. *J Physiol* **117**, 500–544.

Huang H, Wu X, Nicol GD, Meller S & Vasko MR (2003). ATP augments peptide release from rat sensory neurons in culture through activation of P2Y receptors. *J Pharm Exp Ther* **306**, 1137–1144.

Khasar SG, Gold MS & Levine JD (1998). A tetrodotoxin-resistant sodium current mediates inflammatory pain in the rat. *Neurosci Lett* **256**, 17–20.

Khasar SG, Lin YH, Martin A, Dadgar J, McMahon T, Wang D, Hundle B, Aley KO, Isenberg W, McCarter G, Green PG, Hodge CW, Levine JD & Messing RO (1999*a*). A novel nociceptor signaling pathway revealed in protein kinase C ε mutant mice. *Neuron* **24**, 253–260.

Khasar SG, McCarter G & Levine JD (1999*b*). Epinephrine produces a β-adrenergic receptor-mediated mechanical hyperalgesia and in vitro sensitization of rat nociceptors. *J Neurophysiol* **81**, 1104–1112.

Kiernan MC, Baker MD & Bostock H (2003). Characteristics of late Na^+ current in adult rat small sensory neurons. *Neurosci* **119**, 653–660.

Lewis C, Neidhart S, Holy C, North RA, Buell G & Surprenant A (1995). Coexpression of $P2X_2$ and $P2X_3$ receptor subunits can account for ATP-gated currents in sensory neurons. *Nature* **377**, 432–435.

Molliver DC, Cook SP, Carlsten JA, Wright DE & McCleskey EW (2002). ATP and UTP excite sensory neurons and induce CREB phosphorylation through the metabotropic receptor, $P2Y_2$. *Eur J Neurosci* **16**, 1850–1860.

Moriyama T, Iida T, Kobayashi K, Higashi T, Fukuoka T, Tsumura H, Leon C, Suzuki N, Inoue K, Gachet C, Noguchi K & Tominaga M (2003). Possible involvement of $P2Y_2$ metabotropic receptors in ATP-induced transient receptor potential vanilloid receptor 1-mediated thermal hypersensitivity. *J Neurosci* **23**, 6058–6062.

Nakamura F & Strittmatter SM (1996). $P2Y_1$ purinergic receptors in sensory neurons: contribution to touch-induced impulse generation. *Proc Natl Acad Sci U S A* **93**, 10465–10470.

Priest BT, Murphy BA, Lindia JA, Diaz C, Abbadie C, Ritter AM, Liberator P, Iyer LM, Kash SF, Kohler MG, Kaczorowski GJ, Macintyre DE & Martin WJ (2005). Contribution of the tetrodotoxin-resistant voltage-gated sodium channel $Na_V1.9$ to sensory transmission and nociceptive behavior. *Proc Natl Acad Sci U S A* **102**, 9382–9387.

Ralevic V & Burnstock G (1998). Receptors for purines and pyrimidines. *Pharmacol Rev* **50**, 413–492.

Rugiero F, Gola M, Kunze WA, Reynaud JC, Furness JB & Clerc N (2002). Analysis of whole-cell currents by patch clamp of guinea-pig myenteric neurones in intact ganglia. *J Physiol* **538**, 447–463.

Rugiero F, Mistry M, Sage D, Black JA, Waxman SG, Crest M, Clerc N, Delmas P & Gola M (2003). Selective expression of a persistent tetrodotoxin-resistant Na^+ current and $Na_V1.9$ subunit in myenteric sensory neurons. *J Neurosci* **23**, 2715–2725.

Rush AM & Waxman SG (2004). PGE_2 increases the tetrodotoxin-resistant $Na_V1.9$ sodium current in mouse DRG neurons via G-proteins. *Brain Res* **1023**, 264–271.

Sanada M, Yasuda H, Omatsu-Kanbe M, Sango K, Isono T, Matsuura H & Kikkawa R (2002). Increase in intracellular Ca^{2+} and calcitonin gene-related peptide release through metabotropic P2Y receptors in rat dorsal root ganglion neurons. *Neurosci* **111**, 413–422.

Souslova V, Cesare P, Ding Y, Akopian AN, Stanfa L, Suzuki R, Carpenter K, Dickenson A, Boyce S, Hill R, Nebenuis-Oosthuizen D, Smith AJ, Kidd EJ & Wood JN (2000). Warm-coding deficits and aberrant inflammatory pain in mice lacking $P2X_3$ receptors. *Nature* **407**, 1015–1017.

Strassman AM & Raymond SA (1999). Electrophysiological evidence for tetrodotoxin-resistant sodium channels in slowly conducting dural sensory fibers. *J Neurophysiol* **81**, 413–424.

Stucky CL, Medler KA & Molliver DC (2004). The P2Y agonist UTP activates cutaneous afferent fibers. *Pain* **109**, 36–44.

Tominaga M, Wada M & Masu M (2001). Potentiation of capsaicin receptor activity by metabotropic ATP receptors as a possible mechanism for ATP-evoked pain and hyperalgesia. *Proc Natl Acad Sci U S A* **98**, 6951–6956.

Ueno S, Tsuda M, Iwanaga T & Inoue K (1999). Cell type-specific ATP-activated responses in rat dorsal root ganglion neurons. *Br J Pharmacol* **126**, 429–436.

Wang Z, Van Den Berg RJ & Ypey DL (1994). Resting membrane potentials and excitability at different regions of rat dorsal root ganglion neurons in culture. *Neurosci* **60**, 245–254.

Acknowledgements

This work was supported by the MRC and the Wellcome Trust. I am grateful to John Wood for providing me with the $Na_V1.8$ nulls, and for many helpful discussions. I thank Liam Drew, John Wood and Francois Rugiero for reading and commenting on drafts of the manuscript.